Efficient Circuit Simulation of Nonuniform Transmission Lines

Dmitri Kuznetsov

***Abstract*—This paper extends the transmission-line simulation method of [1] to nonuniform lines. The method is applicable to multiconductor lossy frequency-dependent transmission lines characterized by sampled frequency-domain responses. The resulting model can be directly incorporated into a circuit simulator. The implementation includes ac, dc, and transient analyses. The method is reliable, accurate, and as efficient as the simple replacement of interconnects by lumped resistors. The method is based on approximation, and its accuracy and efficiency result from the simplicity of characteristic responses. To apply the method to nonuniform lines, two novel nonuniform line models are introduced. An open-loop model completely separates forward and backward waves and results in the simplest aperiodic responses, but does not guarantee their stability. An open-loop distributed-reflection model explicitly includes the internal distributed reflections, and provides the simplest stable characterization. It is shown that for nonuniform lines, the generalized method of characteristics no longer separates forward and backward waves. Numerical example of a parabolically tapered frequency-dependent four-conductor line is given.**

***Index Terms*—Circuit simulation, interconnect simulation, nonuniform transmission lines, signal-integrity analysis, transient analysis, transmission lines.**

I. Introduction

As the speed of digital circuits increases, the transmission-line behavior of interconnects starts to significantly affect the signal integrity, and their accurate modeling becomes an essential part of the design process. A substantial amount of study has been devoted to the transient simulation of nonuniform transmission lines in recent years [2]–[12]. This paper extends the transmission-line simulation method of [1] to nonuniform lines.

The method can be directly incorporated into a circuit simulator, and supports ac, dc, and transient analyses. For ac and dc analyses, the method uses the Y-parameter element characteristic[1]

$$\begin{cases} \boldsymbol{i}_1(\omega) = \boldsymbol{Y}_{11}(\omega)\boldsymbol{v}_1(\omega) + \boldsymbol{Y}_{12}(\omega)\boldsymbol{v}_2(\omega) \\ \boldsymbol{i}_2(\omega) = \boldsymbol{Y}_{21}(\omega)\boldsymbol{v}_1(\omega) + \boldsymbol{Y}_{22}(\omega)\boldsymbol{v}_2(\omega). \end{cases} \tag{1}$$

For the transient analysis, the method starts with the following frequency-domain element characteristic:

$$\begin{cases} \boldsymbol{i}_1(\omega) = \boldsymbol{Y}_1(\omega)\boldsymbol{v}_1(\omega) - \boldsymbol{j}_1(\omega) \\ \boldsymbol{i}_2(\omega) = \boldsymbol{Y}_2(\omega)\boldsymbol{v}_2(\omega) - \boldsymbol{j}_2(\omega). \end{cases} \tag{2}$$

Then, the matrix admittances $\boldsymbol{Y}_1$ and $\boldsymbol{Y}_2$ and vector current sources $\boldsymbol{j}_1$ and $\boldsymbol{j}_2$ are expressed in terms of transmission-line transfer functions by applying the continuity conditions for the voltages and currents at the line terminals.

To obtain the discrete time-domain element characteristic (needed by the circuit simulator to perform the transient analysis), the transmission-line functions are approximated by rational polynomial functions and then transformed into the discrete time domain using numerical integration. To lower the approximation order and improve the accuracy, the method characterizes transmission lines by open-loop transfer functions, which eliminate reflections from the terminations and provide the simplest stable characterization. As shown in [1], for uniform lines, open-loop characterization is equivalent to the generalized method of characteristics.

The method uses novel rational approximation, indirect numerical integration, and matrix-delay separation techniques. Because the method is based on frequency-domain approximation, it is directly applicable to lines with frequency dependence and lines characterized by measured frequency-domain responses. Since the method introduces neither additional nodes nor current variables, it does not increase the time required for the solution of the circuit equations. As a result, the method has been adopted in several industrial and commercial circuit simulators and, in numerous real-life simulation exercises, proven to be computationally robust. Extensive efficiency and accuracy data, and detailed discussion of alternative transmission-line simulation methods can be found in [1].

The method handles both uniform and nonuniform lines in the same manner. Because of the lack of space, this paper will not repeat the results for uniform lines, but will focus on the differences specific for nonuniform lines. The differences are in the expressions for the Y-parameters in the ac/dc element characteristic (1), and for $\boldsymbol{Y}_1$ and $\boldsymbol{Y}_2$, and $\boldsymbol{j}_1$ and $\boldsymbol{j}_2$ in the transient element characteristic (2). Because the method is based on approximation, its accuracy and efficiency depend on complexity of characteristic responses. This paper presents two models that separate forward and backward waves and provide the simplest characterization for nonuniform lines.

This paper shows that the open-loop model does not guarantee stability of characteristic responses for nonuniform lines, and introduces an open-loop distributed-reflection model which produces the simplest stable characterization. Numerical example demonstrates that both models are in excellent agreement with the analytical solution for multiconductor frequency-dependent parabolically tapered lines of [2].

II. Nonuniform Line Models

A. Open-Loop Model

Nonuniform lines can still be represented by the same system model as uniform lines (see Fig. 1).[2] For nonuniform lines, the propagation functions in the forward and backward directions are no longer the same, and the characteristic admittances become dependent on the position along the line as well as on the direction of wave propagation.

The expressions for $\boldsymbol{Y}_1$ and $\boldsymbol{Y}_2$, and $\boldsymbol{j}_1$ and $\boldsymbol{j}_2$ in the transient element characteristic (2) are derived directly from the continuity conditions for the voltages and currents at the line terminals $\boldsymbol{v}_1 = \boldsymbol{v}_{f1} + \boldsymbol{v}_{b1}$, $\boldsymbol{i}_1 = \boldsymbol{i}_{f1} - \boldsymbol{i}_{b1}$, and the definitions of the characteristic admittances and propagation functions $\boldsymbol{i}_f(x, \omega) = \boldsymbol{Y}_f(x, \omega)\boldsymbol{v}_f(x, \omega)$, $\boldsymbol{i}_{f2}(\omega) = \boldsymbol{W}_{If}(\omega)\boldsymbol{i}_{f1}(\omega)$.[3] Because of the form of the element characteristic (2), it is advantageous to use functions for current waves. To open the feedback loop formed by the reflections from the terminations, the current source $\boldsymbol{j}_1$ must depend only on the backward wave, and $\boldsymbol{j}_2$ only on the forward wave. This condition

Manuscript received September 22, 1995; revised February 13, 1998.

The author is at 347 Massol Ave., Los Gatos, CA 95030 USA (e-mail: vdm@iname.com).

Publisher Item Identifier S 0018-9480(98)03168-8.

[1] Throughout this paper, normal-face, boldface lowercase, and boldface uppercase symbols denote scalars, vectors, and matrices, respectively.

[2] Subscripts "f" and "b" stand for forward and backward waves, "1" and "2" for the near- and far-end terminals, and "V" and "I" for voltage and current functions, respectively.

[3] The corresponding expressions for the backward waves and far-end terminals can be obtained by replacing the subscripts "f" $\leftrightarrow$ "b" and "1" $\leftrightarrow$ "2".

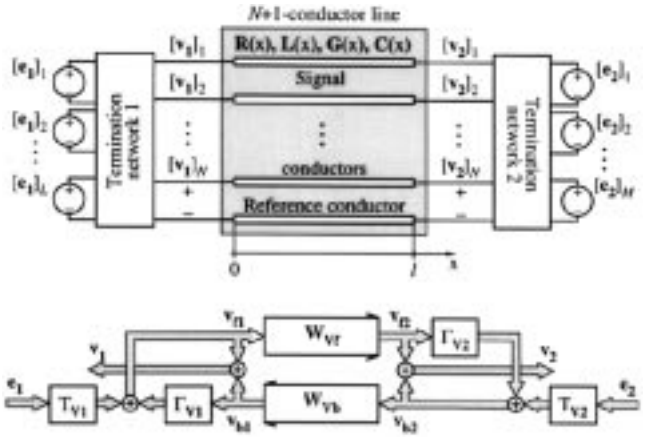

Fig. 1. System diagram representation of a transmission line with terminations. $\boldsymbol{W}_{Vf}$ and $\boldsymbol{W}_{Vb}$ represent the forward and backward matrix propagation functions for voltage waves. $\boldsymbol{T}_{V1}$, $\boldsymbol{T}_{V2}$, and Γ_{V1}, Γ_{V2} stand for the near- and far-end matrix transmission and reflection coefficients.

uniquely defines $\boldsymbol{Y}_1$, $\boldsymbol{Y}_2$, and $\boldsymbol{j}_1$, $\boldsymbol{j}_2$ as follows:

$$\begin{cases} \boldsymbol{Y}_1(\omega) = \boldsymbol{Y}_{f1}(\omega) \\ \boldsymbol{Y}_2(\omega) = \boldsymbol{Y}_{b2}(\omega) \end{cases} \tag{3}$$

$$\begin{cases} \boldsymbol{j}_1(\omega) = \boldsymbol{X}_1(\omega)\boldsymbol{i}_{b1}(\omega) \\ \boldsymbol{j}_2(\omega) = \boldsymbol{X}_2(\omega)\boldsymbol{i}_{f2}(\omega) \end{cases} \tag{4}$$

$$\begin{cases} \boldsymbol{i}_{b1}(\omega) = \boldsymbol{W}_{Ib}(\omega)\boldsymbol{i}_{b2}(\omega) \\ \boldsymbol{i}_{f2}(\omega) = \boldsymbol{W}_{If}(\omega)\boldsymbol{i}_{f1}(\omega) \end{cases}$$

$$\begin{cases} \boldsymbol{i}_{b2}(\omega) = \boldsymbol{i}_2(\omega) + \boldsymbol{i}_{f2}(\omega) \\ \boldsymbol{i}_{f1}(\omega) = \boldsymbol{i}_1(\omega) + \boldsymbol{i}_{b1}(\omega) \end{cases}$$

where $\boldsymbol{X}_1(\omega) = \boldsymbol{I} + \boldsymbol{Y}_{f1}(\omega)\,\boldsymbol{Z}_{b1}(\omega)$, $\boldsymbol{X}_2(\omega) = \boldsymbol{I} + \boldsymbol{Y}_{b2}(\omega)\,\boldsymbol{Z}_{f2}(\omega)$, and $\boldsymbol{Y}_{f1}$, $\boldsymbol{Y}_{b2}$, and $\boldsymbol{Z}_{f2}$, $\boldsymbol{Z}_{b1}$ are forward and backward characteristic admittances and impedances at the near- and far-end terminals. The propagation functions for current waves $\boldsymbol{W}_{If}$ and $\boldsymbol{W}_{Ib}$, are related to the propagation functions for voltage waves, $\boldsymbol{W}_{Vf}$ and $\boldsymbol{W}_{Vb}$, as follows: $\boldsymbol{W}_{If}(\omega) = \boldsymbol{Y}_{f2}(\omega)\boldsymbol{W}_{Vf}(\omega)\boldsymbol{Z}_{f1}(\omega)$ and $\boldsymbol{W}_{Ib}(\omega) = \boldsymbol{Y}_{b1}(\omega)\boldsymbol{W}_{Vb}(\omega)\boldsymbol{Z}_{b2}(\omega)$. As can be seen, for nonuniform lines, the open-loop device model is no longer given by the generalized method of characteristics. However, (3) and (4) cover the generalized method of characteristics [2]–[4] as a special case, in which $\boldsymbol{Y}_{f1} = \boldsymbol{Y}_{f2} = \boldsymbol{Y}_{b1} = \boldsymbol{Y}_{b2} = \boldsymbol{Y}_c$, $\boldsymbol{W}_{If} = \boldsymbol{W}_{Ib}$, and $\boldsymbol{X}_1 = \boldsymbol{X}_2 = 2\boldsymbol{I}$.

By resolving (1)–(4), Y-parameters in the ac/dc element characteristic (1) can be expressed in terms of the open-loop functions (propagation functions and characteristic admittances) as follows:

$$\begin{aligned} \boldsymbol{Y}_{11}(\omega) &= [\boldsymbol{I} + \boldsymbol{X}_1(\omega)\boldsymbol{P}_1^{-1}(\omega)\boldsymbol{W}_{Ib}(\omega)(\boldsymbol{X}_2(\omega) - \boldsymbol{I})\boldsymbol{W}_{If}(\omega)]\boldsymbol{Y}_{f1}(\omega) \\ \boldsymbol{Y}_{12}(\omega) &= -\boldsymbol{X}_1(\omega)\boldsymbol{P}_1^{-1}(\omega)\boldsymbol{W}_{Ib}(\omega)\boldsymbol{Y}_{b2}(\omega) \\ \boldsymbol{Y}_{21}(\omega) &= -\boldsymbol{X}_2(\omega)\boldsymbol{P}_2^{-1}(\omega)\boldsymbol{W}_{If}(\omega)\boldsymbol{Y}_{f1}(\omega) \\ \boldsymbol{Y}_{22}(\omega) &= [\boldsymbol{I} + \boldsymbol{X}_2(\omega)\boldsymbol{P}_2^{-1}(\omega)\boldsymbol{W}_{If}(\omega)(\boldsymbol{X}_1(\omega) - \boldsymbol{I})\boldsymbol{W}_{Ib}(\omega)]\boldsymbol{Y}_{b2}(\omega) \end{aligned} \tag{5}$$

where

$$\boldsymbol{P}_1(\omega) = \boldsymbol{I} - \boldsymbol{W}_{Ib}(\omega)[\boldsymbol{X}_2(\omega) - \boldsymbol{I}]\boldsymbol{W}_{If}(\omega)[\boldsymbol{X}_1(\omega) - \boldsymbol{I}]$$

and

$$\boldsymbol{P}_2(\omega) = \boldsymbol{I} - \boldsymbol{W}_{If}(\omega)[\boldsymbol{X}_1(\omega) - \boldsymbol{I}]\boldsymbol{W}_{Ib}(\omega)[\boldsymbol{X}_2(\omega) - \boldsymbol{I}].$$

The open-loop propagation functions and characteristic admittances for nonuniform lines can be obtained from the general solution of telegrapher's equations by asymptotically separating the terms corresponding to the forward and backward directions of propagation. Table I presents these expressions for parabolically tapered lines.

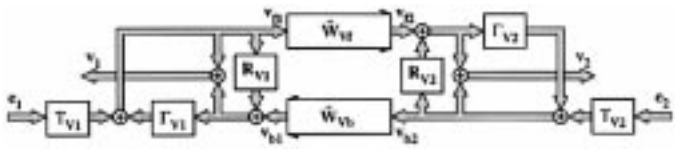

Fig. 2. The internal-reflection system model for nonuniform lines.

Parabolically tapered lines have the simplest analytical solutions, and are convenient to use for testing of nonuniform line models.

As long as a nonuniform line does not have abrupt discontinuities, the open-loop responses are simple aperiodic functions of frequency and time (as they are for uniform lines [1]), and can be accurately represented by a few samples and simulated using a low-order difference approximation with only real poles.

In contrast to uniform lines, the open-loop functions for nonuniform lines, while providing the simplest possible characterization, do not represent distinct physical phenomena which would have to satisfy the energy conservation law. As a result, they can be nonminimum-phase functions[4] with unstable time-domain responses. The reason for this is that in nonuniform lines, the forward and backward waves are coupled via the internal distributed reflections, which are not explicitly included in the open-loop model.

For instance, for parabolically tapered lines, the far-end backward characteristic admittance $\boldsymbol{Y}_{b2}$ is a nonminimum-phase function (see Table I). Nonminimum-phase functions have to be approximated using positive poles which can lead to unacceptably large transient simulation errors. However, for parabolically tapered lines, $\boldsymbol{Y}_{b2}$ is the only nonminimum-phase function in the open-loop element characteristic, and a completely stable characterization can be obtained by premultiplying both sides of the second equation in (2) with $\boldsymbol{Y}_{b2}^{-1}$.

B. Open-Loop Internal-Reflection Model

For a nonuniform-line characterization to be stable in a general case, the line model has to explicitly include the internal distributed reflections. The system-diagram representation of a nonuniform transmission line (taking into account the internal reflections) is shown in Fig. 2.

The near- and far-end internal-reflection coefficients $\boldsymbol{R}_{V1}$ and $\boldsymbol{R}_{V2}$ combine the total effect of the internal distributed reflections produced by the forward wave on its way from the near- to far-end terminal, and by the backward wave on its way from the far- to near-end terminal, respectively.

The internal-reflection propagation functions $\tilde{\boldsymbol{W}}_{Vf}$ and $\tilde{\boldsymbol{W}}_{Vb}$, and reflection coefficients $\boldsymbol{R}_{V1}$ and $\boldsymbol{R}_{V2}$ are identical to the scattering parameters with the matched (at both ends) reference system (as are the propagation functions for uniform lines) and can be directly measured as follows: $\tilde{\boldsymbol{W}}_{Vf} = \boldsymbol{S}_{21}$, $\tilde{\boldsymbol{W}}_{Vb} = \boldsymbol{S}_{12}$, $\boldsymbol{R}_{V1} = \boldsymbol{S}_{11}$, and $\boldsymbol{R}_{V2} = \boldsymbol{S}_{22}$. Table II presents analytical formulas relating the open-loop internal-reflection functions to the open-loop functions.

Because of their distinct physical meaning, the open-loop internal-reflection functions have to satisfy the energy conservation law, and are guaranteed to be stable. The internal-reflection system model in Fig. 2 covers the model in Fig. 1 as a special case in which no internal reflections are present, i.e., $\boldsymbol{R}_{V1} = \boldsymbol{R}_{V2} = 0$. By taking into account internal distributed reflections and eliminating reflections from the terminations, the open-loop internal-reflection functions provide the simplest possible stable characterization for nonuniform lines.

From the internal-reflection system model, we can derive, in the manner similar to the derivation of (3) and (4), the following

[4]Nonminimum-phase functions are transfer functions whose poles are not confined to the left half of the complex plane.

TABLE I
OPEN-LOOP TRANSFER FUNCTIONS FOR PARABOLICALLY TAPERED LINES: $\boldsymbol{Z}(x,\omega)=(1+ax)^2\boldsymbol{Z}(\omega)$, $\boldsymbol{Y}(x,\omega)=(1+ax)^{-2}\boldsymbol{Y}(\omega)$

Name of Function	Function for Current Waves	Function for Voltage Waves
Immittance per unit length	$\mathbf{Y}(\omega)=\mathbf{G}(\omega)+j\omega\mathbf{C}(\omega)$	$\mathbf{Z}(\omega)=\mathbf{R}(\omega)+j\omega\mathbf{L}(\omega)$
Propagation constant	$\mathbf{K_I}(\omega)=\mathbf{Y}(\omega)\mathbf{K_V}(\omega)\mathbf{Y}^{-1}(\omega)=\left[\mathbf{Y}(\omega)\,\mathbf{Z}(\omega)\right]^{\frac{1}{2}}$	$\mathbf{K_V}(\omega)=\mathbf{Z}(\omega)\mathbf{K_I}(\omega)\mathbf{Z}^{-1}(\omega)=\left[\mathbf{Z}(\omega)\,\mathbf{Y}(\omega)\right]^{\frac{1}{2}}$
Propagation delay	$\mathbf{T_I}=\left[\mathbf{C}(\infty)\,\mathbf{L}(\infty)\right]^{\frac{1}{2}}l$	$\mathbf{T_V}=\left[\mathbf{L}(\infty)\,\mathbf{C}(\infty)\right]^{\frac{1}{2}}l$
Propagation function	$\mathbf{W_{If}}(\omega)=\mathbf{Y_{I2}}(\omega)\,\mathbf{W_{Vf}}(\omega)\,\mathbf{Z_{I1}}(\omega)=\hat{\mathbf{W}}_{\mathbf{If}}(\omega)\,\mathbf{e}^{-j\omega\mathbf{T_I}}=\dfrac{1}{1+al}\mathbf{e}^{-\mathbf{K_I}(\omega)\,l}$, $\mathbf{W_{Ib}}(\omega)=\mathbf{Y_{b1}}(\omega)\,\mathbf{W_{Vb}}(\omega)\,\mathbf{Z_{b2}}(\omega)=\hat{\mathbf{W}}_{\mathbf{Ib}}(\omega)\,\mathbf{e}^{-j\omega\mathbf{T_I}}=(1+al)\mathbf{e}^{-\mathbf{K_I}(\omega)\,l}$	$\mathbf{W_{Vf}}(\omega)=\mathbf{Z_{f2}}(\omega)\,\mathbf{W_{If}}(\omega)\,\mathbf{Y_{f1}}(\omega)=\hat{\mathbf{W}}_{\mathbf{Vf}}(\omega)\,\mathbf{e}^{-j\omega\mathbf{T_V}}=\left[\mathbf{I}+\dfrac{1+al}{a}\mathbf{K_V}(\omega)\right]\left\{\left[\mathbf{I}+\dfrac{1}{a}\mathbf{K_V}(\omega)\right]\mathbf{e}^{\mathbf{K_V}(\omega)\,l}\right\}^{-1}$, $\mathbf{W_{Vb}}(\omega)=\mathbf{Z_{b1}}(\omega)\,\mathbf{W_{Ib}}(\omega)\,\mathbf{Y_{b2}}(\omega)=\hat{\mathbf{W}}_{\mathbf{Vb}}(\omega)\,\mathbf{e}^{-j\omega\mathbf{T_V}}=\left[\mathbf{I}-\dfrac{1}{a}\mathbf{K_V}(\omega)\right]\left\{\left[\mathbf{I}-\dfrac{1+al}{a}\mathbf{K_V}(\omega)\right]\mathbf{e}^{\mathbf{K_V}(\omega)\,l}\right\}^{-1}$
Delayless propagation function	$\hat{\mathbf{W}}_{\mathbf{If}}(\omega)=\mathbf{W_{If}}(\omega)\,\mathbf{e}^{j\omega\mathbf{T_I}}$, $\hat{\mathbf{W}}_{\mathbf{Ib}}(\omega)=\mathbf{W_{Ib}}(\omega)\,\mathbf{e}^{j\omega\mathbf{T_I}}$	$\hat{\mathbf{W}}_{\mathbf{Vf}}(\omega)=\mathbf{W_{Vf}}(\omega)\,\mathbf{e}^{j\omega\mathbf{T_V}}$, $\hat{\mathbf{W}}_{\mathbf{Vb}}(\omega)=\mathbf{W_{Vb}}(\omega)\,\mathbf{e}^{j\omega\mathbf{T_V}}$
Characteristic immittance	$\mathbf{Y_{f1}}(\omega)=\mathbf{Z_{f1}^{-1}}(\omega)=\left(\mathbf{K_I}(\omega)+a\mathbf{I}\right)^{-1}\mathbf{Y}(\omega)$, $\mathbf{Y_{b1}}(\omega)=\mathbf{Z_{b1}^{-1}}(\omega)=\left(\mathbf{K_I}(\omega)-a\mathbf{I}\right)^{-1}\mathbf{Y}(\omega)$, $\mathbf{Y_{f2}}(\omega)=\mathbf{Z_{f2}^{-1}}(\omega)=\dfrac{1}{1+al}\left[(1+al)\mathbf{K_I}(\omega)+a\mathbf{I}\right]^{-1}\mathbf{Y}(\omega)$, $\mathbf{Y_{b2}}(\omega)=\mathbf{Z_{b2}^{-1}}(\omega)=\dfrac{1}{1+al}\left[(1+al)\mathbf{K_I}(\omega)-a\mathbf{I}\right]^{-1}\mathbf{Y}(\omega)$	$\mathbf{Z_{f1}}(\omega)=\mathbf{Y_{f1}^{-1}}(\omega)=\left(\mathbf{K_V}(\omega)+a\mathbf{I}\right)\mathbf{Y}^{-1}(\omega)$, $\mathbf{Z_{b1}}(\omega)=\mathbf{Y_{b1}^{-1}}(\omega)=\left(\mathbf{K_V}(\omega)-a\mathbf{I}\right)\mathbf{Y}^{-1}(\omega)$, $\mathbf{Z_{f2}}(\omega)=\mathbf{Y_{f2}^{-1}}(\omega)=(1+al)\left[(1+al)\mathbf{K_V}(\omega)+a\mathbf{I}\right]\mathbf{Y}^{-1}(\omega)$, $\mathbf{Z_{b2}}(\omega)=\mathbf{Y_{b2}^{-1}}(\omega)=(1+al)\left[(1+al)\mathbf{K_V}(\omega)-a\mathbf{I}\right]\mathbf{Y}^{-1}(\omega)$

Note: The subscripts "*f*", "*b*", "*V*", "*I*", "1" and "2" refer to the forward and backward voltage and current waves at the near and far-end terminals, respectively.

expressions for $\boldsymbol{Y}_1$ and $\boldsymbol{Y}_2$, and $\boldsymbol{j}_1$ and $\boldsymbol{j}_2$ in the transient element characteristic (2):

$$\begin{cases}\boldsymbol{Y}_1(\omega)=[\boldsymbol{X}_1(\omega)-\boldsymbol{I}]\boldsymbol{Y}_{c1}(\omega)\\ \boldsymbol{Y}_2(\omega)=[\boldsymbol{X}_2(\omega)-\boldsymbol{I}]\boldsymbol{Y}_{c2}(\omega)\end{cases}\tag{6}$$

$$\begin{cases}\boldsymbol{j}_1(\omega)=\boldsymbol{X}_1(\omega)\boldsymbol{i}_{b1}(\omega)\\ \boldsymbol{j}_2(\omega)=\boldsymbol{X}_2(\omega)\boldsymbol{i}_{f2}(\omega)\end{cases}\tag{7}$$

$$\begin{cases}\boldsymbol{i}_{b1}(\omega)=\tilde{\boldsymbol{W}}_{Ib}(\omega)\boldsymbol{i}_{b2}(\omega)\\ \boldsymbol{i}_{f2}(\omega)=\tilde{\boldsymbol{W}}_{If}(\omega)\boldsymbol{i}_{f1}(\omega)\end{cases}$$

$$\begin{cases}\boldsymbol{i}_{b2}(\omega)=[\boldsymbol{I}-\boldsymbol{R}_{I2}(\omega)]^{-1}[\boldsymbol{i}_2(\omega)+\boldsymbol{i}_{f2}(\omega)]\\ \boldsymbol{i}_{f1}(\omega)=[\boldsymbol{I}-\boldsymbol{R}_{I1}(\omega)]^{-1}[\boldsymbol{i}_1(\omega)+\boldsymbol{i}_{b1}(\omega)]\end{cases}$$

where $\boldsymbol{X}_1(\omega)=\boldsymbol{I}+[\boldsymbol{I}-\boldsymbol{R}_{I1}(\omega)][\boldsymbol{I}+\boldsymbol{R}_{I1}(\omega)]^{-1}$ and $\boldsymbol{X}_2(\omega)=\boldsymbol{I}+[\boldsymbol{I}-\boldsymbol{R}_{I2}(\omega)][\boldsymbol{I}+\boldsymbol{R}_{I2}(\omega)]^{-1}$. The near- and far-end characteristic admittances $\boldsymbol{Y}_{c1}$ and $\boldsymbol{Y}_{c2}$ are equal to the characteristic admittances of uniform lines with the same values of distributed parameters as those of the nonuniform line at the ends, and do not depend on the direction of propagation. The propagation functions and internal reflection coefficients for current waves $\tilde{\boldsymbol{W}}_{If}$, $\tilde{\boldsymbol{W}}_{Ib}$, $\boldsymbol{R}_{I1}$, and $\boldsymbol{R}_{I2}$ are related to the propagation functions and internal reflection coefficients for voltage waves $\tilde{\boldsymbol{W}}_{Vf}$, $\tilde{\boldsymbol{W}}_{Vb}$, $\boldsymbol{R}_{V1}$, and $\boldsymbol{R}_{V2}$ as follows: $\tilde{\boldsymbol{W}}_{If}(\omega)=\boldsymbol{Y}_{c2}(\omega)\tilde{\boldsymbol{W}}_{Vf}(\omega)\boldsymbol{Z}_{c1}(\omega)$, $\tilde{\boldsymbol{W}}_{Ib}(\omega)=\boldsymbol{Y}_{c1}(\omega)\tilde{\boldsymbol{W}}_{Vb}(\omega)\boldsymbol{Z}_{c2}(\omega)$, $\boldsymbol{R}_{I1}(\omega)=\boldsymbol{Y}_{c1}(\omega)\boldsymbol{R}_{V1}(\omega)\boldsymbol{Z}_{c1}(\omega)$, and $\boldsymbol{R}_{I2}(\omega)=\boldsymbol{Y}_{c2}(\omega)\boldsymbol{R}_{V2}(\omega)\boldsymbol{Z}_{c2}(\omega)$. Equations (6) and (7) cover the generalized method of characteristics as a special case in which $\boldsymbol{Y}_{c1}=\boldsymbol{Y}_{c2}=\boldsymbol{Y}_c$, $\boldsymbol{W}_{If}=\boldsymbol{W}_{Ib}$, $\boldsymbol{R}_{V1}=\boldsymbol{R}_{V2}=0$, and $\boldsymbol{X}_1=\boldsymbol{X}_2=2\boldsymbol{I}$.

For practical application, its is advantageous to combine (6) and (7) and to express them in terms of the terminal voltages instead of the currents

$$\begin{cases}\boldsymbol{j}_1(\omega)=\boldsymbol{H}_{Ib}(\omega)[\boldsymbol{X}_2(\omega)\boldsymbol{Y}_{c2}(\omega)\boldsymbol{v}_2(\omega)-\boldsymbol{j}_2(\omega)]\\ \boldsymbol{j}_2(\omega)=\boldsymbol{H}_{If}(\omega)[\boldsymbol{X}_1(\omega)\boldsymbol{Y}_{c1}(\omega)\boldsymbol{v}_1(\omega)-\boldsymbol{j}_1(\omega)]\end{cases}$$

where

$$\boldsymbol{H}_{Ib}(\omega)=\boldsymbol{X}_1(\omega)\tilde{\boldsymbol{W}}_{Ib}(\omega)[\boldsymbol{I}+\boldsymbol{R}_{I2}(\omega)]^{-1}\boldsymbol{X}_2^{-1}(\omega)$$

and

$$\boldsymbol{H}_{If}(\omega)=\boldsymbol{X}_2(\omega)\tilde{\boldsymbol{W}}_{If}(\omega)[\boldsymbol{I}+\boldsymbol{R}_{I1}(\omega)]^{-1}\boldsymbol{X}_1^{-1}(\omega).$$

This way, the terminal currents do not have to be recovered.

The transfer functions $\boldsymbol{H}_{If}$ and $\boldsymbol{H}_{Ib}$ contain delays which originate from the propagation functions $\tilde{\boldsymbol{W}}_{If}$ and $\tilde{\boldsymbol{W}}_{Ib}$. Before the difference approximation is applied, the delays are separated via the matrix delay separation technique, which represents the matrix transfer functions in the following form:

$$\boldsymbol{H}_{If}(\omega)=\hat{\boldsymbol{H}}_{If}(\omega)\boldsymbol{M}_{If}e^{-j\omega\boldsymbol{T}_{Ifm}}\boldsymbol{M}_{If}^{-1}$$

$$\boldsymbol{H}_{Ib}(\omega)=\hat{\boldsymbol{H}}_{Ib}(\omega)M_{Ib}e^{-j\omega\boldsymbol{T}_{IBm}}\boldsymbol{M}_{Ib}^{-1}$$

where the delayless transfer functions $\hat{\boldsymbol{H}}_{If}$ and $\hat{\boldsymbol{H}}_{Ib}$ are found as

$$\hat{\boldsymbol{H}}_{If}(\omega)=\boldsymbol{H}_{If}(\omega)e^{j\omega\boldsymbol{T}_{If}}$$

$$\hat{\boldsymbol{H}}_{Ib}(\omega)=\boldsymbol{H}_{Ib}(\omega)e^{j\omega\boldsymbol{T}_{Ib}}.$$

The matrix propagation delays $\boldsymbol{T}_{If}$ and $\boldsymbol{T}_{Ib}$ are the same in the forward and backward directions: $\boldsymbol{T}_{If}=\boldsymbol{T}_{Ib}=\boldsymbol{T}_I$, and are equal for all of $\boldsymbol{W}_{If}$, $\boldsymbol{W}_{Ib}$, $\tilde{\boldsymbol{W}}_{If}$, $\tilde{\boldsymbol{W}}_{Ib}$, $\boldsymbol{H}_{If}$, and $\boldsymbol{H}_{Ib}$. $\boldsymbol{T}_{Ifm}$ and $\boldsymbol{T}_{IBm}$,

TABLE II
EXPRESSIONS FOR THE OPEN-LOOP INTERNAL-REFLECTION FUNCTIONS IN TERMS OF THE OPEN-LOOP FUNCTIONS

Name of Function	Function for Current Waves	Function for Voltage Waves
Propagation function	$\tilde{\mathbf{W}}_{If}(\omega)=\mathbf{Y}_{c2}(\omega)\tilde{\mathbf{W}}_{Vf}(\omega)\mathbf{Z}_{c1}(\omega)=\mathbf{T}_{I22}(\omega)\mathbf{W}_{If}(\omega)\cdot\left[\mathbf{I}-\Gamma_{I12}(\omega)\mathbf{W}_{Ib}(\omega)\Gamma_{I22}(\omega)\mathbf{W}_{If}(\omega)\right]^{-1}\mathbf{T}_{I11}(\omega)$, $\tilde{\mathbf{W}}_{Ib}(\omega)=\mathbf{Y}_{c1}(\omega)\tilde{\mathbf{W}}_{Vb}(\omega)\mathbf{Z}_{c2}(\omega)=\mathbf{T}_{I12}(\omega)\mathbf{W}_{Ib}(\omega)\cdot\left[\mathbf{I}-\Gamma_{I22}(\omega)\mathbf{W}_{If}(\omega)\Gamma_{I12}(\omega)\mathbf{W}_{Ib}(\omega)\right]^{-1}\mathbf{T}_{I21}(\omega)$	$\tilde{\mathbf{W}}_{Vf}(\omega)=\mathbf{Z}_{c2}(\omega)\tilde{\mathbf{W}}_{If}(\omega)\mathbf{Y}_{c1}(\omega)=\mathbf{T}_{V22}(\omega)\mathbf{W}_{Vf}(\omega)\cdot\left[\mathbf{I}-\Gamma_{V12}(\omega)\mathbf{W}_{Vb}(\omega)\Gamma_{V22}(\omega)\mathbf{W}_{Vf}(\omega)\right]^{-1}\mathbf{T}_{V11}(\omega)$, $\tilde{\mathbf{W}}_{Vb}(\omega)=\mathbf{Z}_{c1}(\omega)\tilde{\mathbf{W}}_{Ib}(\omega)\mathbf{Y}_{c2}(\omega)=\mathbf{T}_{V12}(\omega)\mathbf{W}_{Vb}(\omega)\cdot\left[\mathbf{I}-\Gamma_{V22}(\omega)\mathbf{W}_{Vf}(\omega)\Gamma_{V12}(\omega)\mathbf{W}_{Vb}(\omega)\right]^{-1}\mathbf{T}_{V21}(\omega)$
Internal reflection coefficient	$\mathbf{R}_{I1}(\omega)=\mathbf{Y}_{c1}(\omega)\mathbf{R}_{V1}(\omega)\mathbf{Z}_{c1}(\omega)=\Gamma_{I11}(\omega)+\mathbf{T}_{I12}(\omega)\mathbf{W}_{Ib}(\omega)\Gamma_{I22}(\omega)\mathbf{W}_{If}(\omega)\cdot\left[\mathbf{I}-\Gamma_{I12}(\omega)\mathbf{W}_{Ib}(\omega)\Gamma_{I22}(\omega)\mathbf{W}_{If}(\omega)\right]^{-1}\mathbf{T}_{I11}(\omega)$, $\mathbf{R}_{I2}(\omega)=\mathbf{Y}_{c2}(\omega)\mathbf{R}_{V2}(\omega)\mathbf{Z}_{c2}(\omega)=\Gamma_{I21}(\omega)+\mathbf{T}_{I22}(\omega)\mathbf{W}_{If}(\omega)\Gamma_{I12}(\omega)\mathbf{W}_{Ib}(\omega)\cdot\left[\mathbf{I}-\Gamma_{I22}(\omega)\mathbf{W}_{If}(\omega)\Gamma_{I12}(\omega)\mathbf{W}_{Ib}(\omega)\right]^{-1}\mathbf{T}_{I21}(\omega)$	$\mathbf{R}_{V1}(\omega)=\mathbf{Z}_{c1}(\omega)\mathbf{R}_{I1}(\omega)\mathbf{Y}_{c1}(\omega)=\Gamma_{V11}(\omega)+\mathbf{T}_{V12}(\omega)\mathbf{W}_{Vb}(\omega)\Gamma_{V22}(\omega)\mathbf{W}_{Vf}(\omega)\cdot\left[\mathbf{I}-\Gamma_{V12}(\omega)\mathbf{W}_{Vb}(\omega)\Gamma_{V22}(\omega)\mathbf{W}_{Vf}(\omega)\right]^{-1}\mathbf{T}_{V11}(\omega)$, $\mathbf{R}_{V2}(\omega)=\mathbf{Z}_{c2}(\omega)\mathbf{R}_{I2}(\omega)\mathbf{Y}_{c2}(\omega)=\Gamma_{V21}(\omega)+\mathbf{T}_{V22}(\omega)\mathbf{W}_{Vf}(\omega)\Gamma_{V12}(\omega)\mathbf{W}_{Vb}(\omega)\cdot\left[\mathbf{I}-\Gamma_{V22}(\omega)\mathbf{W}_{Vf}(\omega)\Gamma_{V12}(\omega)\mathbf{W}_{Vb}(\omega)\right]^{-1}\mathbf{T}_{V21}(\omega)$
Characteristic immittance	$\mathbf{Y}_{c1}(\omega)=\mathbf{Z}_{c1}^{-1}(\omega)=\left[\mathbf{Y}(0,\omega)\mathbf{Z}(0,\omega)\right]^{\frac{1}{2}}\mathbf{Z}^{-1}(0,\omega)$, $\mathbf{Y}_{c2}(\omega)=\mathbf{Z}_{c2}^{-1}(\omega)=\left[\mathbf{Y}(l,\omega)\mathbf{Z}(l,\omega)\right]^{\frac{1}{2}}\mathbf{Z}^{-1}(l,\omega)$	$\mathbf{Z}_{c1}(\omega)=\mathbf{Y}_{c1}^{-1}(\omega)=\left[\mathbf{Z}(0,\omega)\mathbf{Y}(0,\omega)\right]^{\frac{1}{2}}\mathbf{Y}^{-1}(0,\omega)$, $\mathbf{Z}_{c2}(\omega)=\mathbf{Y}_{c2}^{-1}(\omega)=\left[\mathbf{Z}(l,\omega)\mathbf{Y}(l,\omega)\right]^{\frac{1}{2}}\mathbf{Y}^{-1}(l,\omega)$
Transmission coefficient	$\mathbf{T}_{I11}(\omega)=2\left[\mathbf{I}+\mathbf{Y}_{c1}(\omega)\mathbf{Z}_{f1}(\omega)\right]^{-1}$, $\mathbf{T}_{I12}(\omega)=\left[\mathbf{I}+\mathbf{Y}_{f1}(\omega)\mathbf{Z}_{c1}(\omega)\right]^{-1}\left[\mathbf{I}+\mathbf{Y}_{f1}(\omega)\mathbf{Z}_{b1}(\omega)\right]$, $\mathbf{T}_{I21}(\omega)=2\left[\mathbf{I}+\mathbf{Y}_{c2}(\omega)\mathbf{Z}_{b2}(\omega)\right]^{-1}$, $\mathbf{T}_{I22}(\omega)=\left[\mathbf{I}+\mathbf{Y}_{b2}(\omega)\mathbf{Z}_{c2}(\omega)\right]^{-1}\left[\mathbf{I}+\mathbf{Y}_{b2}(\omega)\mathbf{Z}_{f2}(\omega)\right]$	$\mathbf{T}_{V11}(\omega)=2\left[\mathbf{I}+\mathbf{Z}_{c1}(\omega)\mathbf{Y}_{f1}(\omega)\right]^{-1}$, $\mathbf{T}_{V12}(\omega)=\left[\mathbf{I}+\mathbf{Z}_{f1}(\omega)\mathbf{Y}_{c1}(\omega)\right]^{-1}\left[\mathbf{I}+\mathbf{Z}_{f1}(\omega)\mathbf{Y}_{b1}(\omega)\right]$, $\mathbf{T}_{V21}(\omega)=2\left[\mathbf{I}+\mathbf{Z}_{c2}(\omega)\mathbf{Y}_{b2}(\omega)\right]^{-1}$, $\mathbf{T}_{V22}(\omega)=\left[\mathbf{I}+\mathbf{Z}_{b2}(\omega)\mathbf{Y}_{c2}(\omega)\right]^{-1}\left[\mathbf{I}+\mathbf{Z}_{b2}(\omega)\mathbf{Y}_{f2}(\omega)\right]$
Reflection coefficient	$\Gamma_{I11}(\omega)=\left[\mathbf{I}+\mathbf{Y}_{f1}(\omega)\mathbf{Z}_{c1}(\omega)\right]^{-1}\left[\mathbf{I}-\mathbf{Y}_{f1}(\omega)\mathbf{Z}_{c1}(\omega)\right]$, $\Gamma_{I12}(\omega)=\left[\mathbf{I}+\mathbf{Y}_{c1}(\omega)\mathbf{Z}_{f1}(\omega)\right]^{-1}\left[\mathbf{I}-\mathbf{Y}_{c1}(\omega)\mathbf{Z}_{b1}(\omega)\right]$, $\Gamma_{I21}(\omega)=\left[\mathbf{I}+\mathbf{Y}_{b2}(\omega)\mathbf{Z}_{c2}(\omega)\right]^{-1}\left[\mathbf{I}-\mathbf{Y}_{b2}(\omega)\mathbf{Z}_{c2}(\omega)\right]$, $\Gamma_{I22}(\omega)=\left[\mathbf{I}+\mathbf{Y}_{c2}(\omega)\mathbf{Z}_{b2}(\omega)\right]^{-1}\left[\mathbf{I}-\mathbf{Y}_{c2}(\omega)\mathbf{Z}_{f2}(\omega)\right]$	$\Gamma_{V11}(\omega)=\left[\mathbf{I}+\mathbf{Z}_{f1}(\omega)\mathbf{Y}_{c1}(\omega)\right]^{-1}\left[\mathbf{Z}_{f1}(\omega)\mathbf{Y}_{c1}(\omega)-\mathbf{I}\right]$, $\Gamma_{V12}(\omega)=\left[\mathbf{I}+\mathbf{Z}_{c1}(\omega)\mathbf{Y}_{f1}(\omega)\right]^{-1}\left[\mathbf{Z}_{c1}(\omega)\mathbf{Y}_{b1}(\omega)-\mathbf{I}\right]$, $\Gamma_{V21}(\omega)=\left[\mathbf{I}+\mathbf{Z}_{b2}(\omega)\mathbf{Y}_{c2}(\omega)\right]^{-1}\left[\mathbf{Z}_{b2}(\omega)\mathbf{Y}_{c2}(\omega)-\mathbf{I}\right]$, $\Gamma_{V22}(\omega)=\left[\mathbf{I}+\mathbf{Z}_{c2}(\omega)Y_{b2}(\omega)\right]^{-1}\left[\mathbf{Z}_{c2}(\omega)\mathbf{Y}_{f2}(\omega)-\mathbf{I}\right]$

and $\boldsymbol{M}_{If}$ and $\boldsymbol{M}_{Ib}$ are diagonal eigenvalue and constant eigenvector matrices of $\boldsymbol{T}_{If}$ and $\boldsymbol{T}_{Ib}$, respectively.

The Y-parameters in the ac/dc model (1) are expressed in terms of the internal-reflection functions as follows:

$$\begin{aligned}
\boldsymbol{Y}_{11}(\omega) &= \{\boldsymbol{X}_1(\omega)[\boldsymbol{I}+\boldsymbol{P}_1^{-1}(\omega)\tilde{\boldsymbol{W}}_{Ib}(\omega)\\
&\qquad\cdot(\boldsymbol{I}+\boldsymbol{R}_{I2}(\omega))\tilde{\boldsymbol{W}}_{If}(\omega)]-\boldsymbol{I}\}\boldsymbol{Y}_{c1}(\omega)\\
\boldsymbol{Y}_{12}(\omega) &= -\boldsymbol{X}_1(\omega)\boldsymbol{P}_1^{-1}(\omega)\tilde{\boldsymbol{W}}_{Ib}(\omega)\boldsymbol{Y}_{c2}(\omega)\\
\boldsymbol{Y}_{21}(\omega) &= -\boldsymbol{X}_2(\omega)\boldsymbol{P}_2^{-1}(\omega)\tilde{\boldsymbol{W}}_{If}(\omega)\boldsymbol{Y}_{c1}(\omega)\\
\boldsymbol{Y}_{22}(\omega) &= \{\boldsymbol{X}_2(\omega)[\boldsymbol{I}+\boldsymbol{P}_2^{-1}(\omega)\tilde{\boldsymbol{W}}_{If}(\omega)\\
&\qquad\cdot(\boldsymbol{I}+\boldsymbol{R}_{I1}(\omega))\tilde{\boldsymbol{W}}_{Ib}(\omega)]-\boldsymbol{I}\}\boldsymbol{Y}_{c2}(\omega)
\end{aligned}$$

where

$$\boldsymbol{P}_1(\omega)=\boldsymbol{I}-\tilde{\boldsymbol{W}}_{Ib}(\omega)[\boldsymbol{I}+\boldsymbol{R}_{I2}(\omega)]\tilde{\boldsymbol{W}}_{If}(\omega)[\boldsymbol{I}+\boldsymbol{R}_{I1}(\omega)])$$

and

$$\boldsymbol{P}_2(\omega)=\boldsymbol{I}-\tilde{\boldsymbol{W}}_{If}(\omega)[\boldsymbol{I}+\boldsymbol{R}_{I1}(\omega)]\tilde{\boldsymbol{W}}_{Ib}(\omega)[\boldsymbol{I}+\boldsymbol{R}_{I2}(\omega)].$$

Because they include the distributed feedback due to the internal reflections, the open-loop internal-reflection functions are more complicated than the open-loop functions. Consequently, they require a higher order approximation and have to be approximated using both real and complex poles. However, because the reflections from the terminations are eliminated, the open-loop internal-reflection transfer functions do not contain nondecaying oscillations (provided that the nonuniform line does not contain abrupt discontinuities inside), and still can be approximated in the full range from zero to infinity.

Distributed-reflection functions typically require 15–30-order approximation for the full frequency/time range (in contrast to the 3–10-order approximation for the open-loop functions). However, the open-loop internal-reflection characterization is still simpler than any other stable characterization (such as S-, Y-, Z-, or H-parameters) because it is the only characterization that opens the feedback loop formed by reflections from the terminations.

III. NUMERICAL RESULTS

The accuracy and reliability of the method have been tested in numerous simulation exercises. Fig. 3 shows transient waveforms for the four-conductor parabolically tapered frequency-dependent line of [2] simulated with the open-loop and open-loop internal-reflection

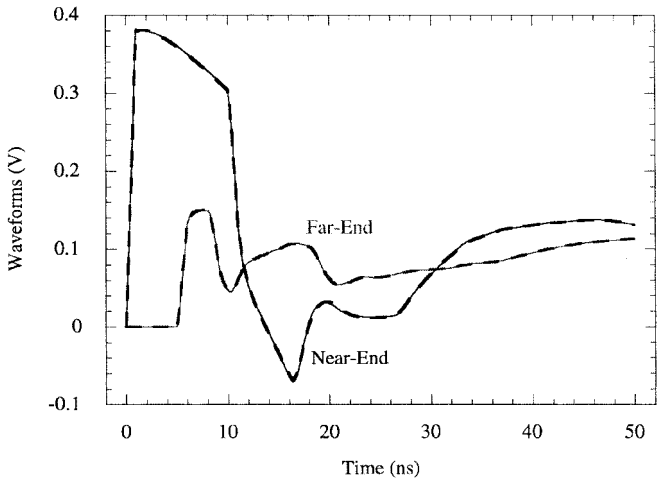

Fig. 3. Transient waveforms at conductor 3 of the four-conductor frequency-dependent parabolically tapered line of [2]. Thin continuous curves show the results obtained with the open-loop model and thick dashed curves show those for the open-loop internal-reflection model.

models installed in a modified nodal approach (MNA)-based circuit simulator. The results are in excellent agreement with the analytical solutions in [2, p. 12, Fig. 4(a) and (b)]. Seventh-order real-pole approximation was used for the open-loop model, and a 17th-order complex-pole approximation was used for the open-loop internal-reflection model.

The run-time comparisons for circuits of various sizes and types can be found in [1]. The run-time data in [1] were obtained with the open-loop nonuniform line model.

IV. Conclusions

This paper presented the application of the transmission-line simulation method [1] to nonuniform lines. Two novel nonuniform line models were introduced.

The open-loop model results in the simplest aperiodic responses (similar to those for uniform lines), which can be accurately represented by a few samples and a low-order approximation with only real poles. The model, however, does not guarantee stability of the line characterization.

The open-loop internal-reflection model provides the simplest stable characterization, which is, however, more complex than the open-loop characterization and requires a higher order approximation with complex poles.

References

[1] D. B. Kuznetsov and J. E. Schutt-Ainé, "Optimal transient simulation of transmission lines," *IEEE Trans. Circuits Syst. I*, vol. 43, pp. 111–121, Feb. 1996.

[2] F.-Y. Chang, "Transient simulation of frequency-dependent nonuniform coupled lossy transmission lines," *IEEE Trans. Comp., Packag., Manufact. Technol.*, vol. 17, pp. 3–14, Feb. 1994.

[3] ——, "Transient simulation of nonuniform coupled lossy transmission lines characterized with frequency-dependent parameters, Part I: Waveform relaxation analysis," *IEEE Trans. Circuits Syst. I*, vol. 39, pp. 582–603, Aug. 1992.

[4] ——, "Transient simulation of nonuniform coupled lossy transmission lines characterized with frequency-dependent parameters, Part II: Discrete-time analysis," *IEEE Trans. Circuits Syst. I*, vol. 39, pp. 907–927, Nov. 1992.

[5] M. T. Correia de Barrosand and M. E. Almeida, "Computation of electromagnetic transients on nonuniform transmission lines," *IEEE Trans. Power Delivery*, vol. 11, pp. 1082–1091, Apr. 1996.

[6] J.-F. Mao and Z.-F. Li, "Waveform relaxation solution of the $ABCD$ matrices of nonuniform transmission lines for transient analysis," *IEEE Trans. Computer-Aided Design*, vol. 13, pp. 1409–1412, Nov. 1994.

[7] A. S. Al Fuhaid, "s-domain analysis of electromagnetic transients on nonuniform lines," *IEEE Trans. Power Delivery*, vol. 5, pp. 2072–2083, Nov. 1990.

[8] S. He, "Frequency and time domain green function technique for nonuniform *LCRG* transmission lines with frequency-dependent parameters," *J. Electromagnetic Waves Applicat.*, vol. 7, pp. 31–38, 1993.

[9] C. Hsue and C. C. Hechtman, "Transient analysis of nonuniform, high-pass transmission lines," *IEEE Trans. Microwave Theory Tech.*, vol. 38, pp. 1023–1030, Aug. 1990.

[10] O. A. Palusinski and A. Lee, "Analysis of transients in nonuniform and uniform multiconductor transmission lines," *IEEE Trans. Microwave Theory Tech.*, vol. 37, pp. 127–138, Jan. 1989.

[11] Y.-C. Yang, J. A. Kong, and Q. Gu, "Time-domain perturbation analysis of nonuniformly coupled transmission lines," *IEEE Trans. Microwave Theory Tech.*, vol. MTT-33, pp. 1120–1130, Nov. 1985.

[12] J. L. Hill and D. Mathews, "Transient analysis of systems with exponential transmission lines," *IEEE Trans. Microwave Theory Tech.*, vol. MTT-25, pp. 777–783, Sept. 1977.

Micromachined Thermocouple Microwave Detector by Commercial CMOS Fabrication

Veljko Milanović, Michael Gaitan, and Mona E. Zaghloul

***Abstract*— This paper reports on the design and testing of a thermocouple microwave detector fabricated through a commercial CMOS foundry with an additional maskless etching procedure. The detector measures true rms power of signals in the frequency range from 50 MHz to 20 GHz, and input power range from −30 to +10 dBm. The device has linearity better than ±0.4% for input power versus output voltage over the 40-dB dynamic range. Measurements of the return loss, obtained using an automatic network analyzer, show acceptable input return loss of less than −20 dB over the entire frequency range. The sensitivity of the detector was measured to be (1.007 ±0.004) mV/mW.**

I. Introduction

Thermocouple-based power sensors have been one of the most widely used tools for microwave power detection [1]–[4].[1] These sensors employ a simple principle of conversion of electric power to thermal power, which is then indirectly measured.[2] A terminating resistor dissipates the microwave energy in the form of heat. The measurement of the temperature differential caused by the resistive

Manuscript received May 6, 1996; revised February 13, 1998. This work was supported by the Naval Command, Control and Ocean Surveillance Center, RDT&E DIV, San Diego, CA. The work of V. Milanović was supported by RF Microsystems, San Diego, CA.

V. Milanović and M. E. Zaghloul are with the Department of Electrical Engineering and Computer Science, The George Washington University, Washington, DC 20052 (e-mail: veljko@seas.gwu.edu) USA.

M. Gaitan is with the Semiconductor Electronics Division, National Institute of Standards and Technology, Gaithersburg, MD 20899 USA.

Publisher Item Identifier S 0018-9480(98)03154-8.

[1] Hewlett-Packard Co., "Fundamentals of RF and microwave power measurement," *Applicat. Note AN 64-1*, June 1978.

[2] J. R. Kinard, J. R. Hastings, T. E. Lipe, and C. B. Childers, *AC–DC Difference Calibration.* NIST Special Publication, vol. 250-27, May 1989.